Identification of native co-factors of MshB and MCA from *Mycobacterium* species

Evren Kocabas

Thesis submitted to the faculty of

Virginia Polytechnic Institute and State University

in partial fulfillment of the requirements for the degree of

Master of Science in Life Sciences

In

Biochemistry

Marcy Hernick, Chair

Michael Wade Klemba, Committee Member

Richard F Helm, Committee Member

August 11, 2010

Blacksburg, Virginia

Keywords: MshB, MCA, metal-dependent deacetylase, *Mycobacterium tuberculosis, Mycobacterium smegmatis*, iron, zinc

Copyright 2010, Evren Kocabas

Identification of native co-factors of MshB and MCA from *Mycobacterium* species

Evren Kocabas

Marcy Hernick, Chair

Department of Biochemistry

ABSTRACT

Mycothiol (MSH), a low-molecular- weight thiol, is a primary reducing agent and essential for the survival of mycobacteria. The full pathway of MSH biosynthesis and detoxification includes various promising drug targets. Several metalloenzymes are involved in this pathway, such as a deacetylase (MshB) and mycothiol *S*-conjugate amidase (MCA). MshB catalyzes the deacetylation of GlcNAc-Ins to form GlcN-Ins and acetate. Mycothiol *S*-conjugate amidase (MCA) cleaves the amide bond of mycothiol *S*-conjugates of various drugs and toxins. The identification of the native co-factor is critical for the design of potent and effective inhibitors. Therefore, in this study, we identified the possible native co-factors of MshB and MCA from *M. smegmatis* and *M. tuberculosis*.

To reach our aim, we used a pull-down method to rapidly purify halo-MshB and halo-MCA under anaerobic conditions. Our data indicates that the metal bound to MshB and MCA anaerobically purified from *E. coli* grown in minimal medium is mainly Fe(II), while proteins purified under aerobic conditions contain bound Zn (II) and Fe(II) that varies with the metal content of the medium. For a further clarification of the metal ion preferences of MshB and MCA, we determined the MshB and MCA affinity for Zn(II) to be in the picomolar range and *Ms* MshB affinity for Fe(II) in nanomolar range. These results indicate that MshB and MCA can be found bound with either iron or zinc and this is independent to their affinities for these metal ions.

TABLE OF CONTENTS

ABSTRACT ..... **ii**

TABLE OF CONTENTS ..... **iii**

LIST OF FIGURES and LIST OF TABLES ..... **iv**

ACKNOWLEDGEMENT ..... **v**

CHAPTER ONE: INTRODUCTION **1**

CHAPTER TWO: PULL-DOWN EXPERIMENTS WITH HALO-MshB AND MCA **18**

I. Introduction **18**

II. Materials and Methods **19**

III. Results **24**

IV. Discussion **29**

CHAPTER THREE: *MYCOBACTERIAL* MshB AND MCA METAL ION AFFINITY MEASUREMENTS **33**

I. Introduction **33**

II. Materials and Methods **34**

III. Results **43**

IV. Discussion **50**

CHAPTER FOUR: CONCLUDING REMARKS AND FUTURE DIRECTIONS **53**

REFERENCE LIST **57**

LIST OF FIGURES

Chapter One

1.1 The Biosynthesis and Detoxification Pathway of Mycothiol 16

1.2 A proposed catalytic mechanism for MshB 17

Chapter Two

2.1 Schematic of the pFN18K HaloTag® T7 Flexi® expression vector 26

2.2 Pull-down experiment of *Ms* MshB.....27

2.3 Comparison of metal content of MshB and MCA were isolated from *E. coli* aerobically and anaerobically 28

Chapter Three

3.1 Schematic of the pVP56K expression vector 45

3.2 $K_D^{Fe(II)}$ and $K_D^{Zn(II)}$ values for *Ms* MshB 48

LIST OF TABLES

Chapter Three

3.1 Results of the expression and purification of apo-*Mt* MshB 45

3.2 The amounts of total and free iron buffers used in affinity assays 46

3.3 The amounts of total and free zinc buffers used in affinity assays.....47

3.4 $K_D^{Fe(II)}$ and $K_D^{Zn(II)}$ values for MshB and MCA 49

ACKNOWLEDGEMENTS

I would like to thank my advisor, Dr. Marcy Hernick, for her assistance, patience during my graduate research and welcoming me to her lab as her first graduate student.

I am very thankful to the members of my graduate committee, Dr. Michael Klemba, Dr. Richard Helm and Dr. Pablo Sobrado for their time, patience, and advice for my personal and scientific improvement.

I would like to thank to the past and present members of the Hernick Laboratory: Hualan Lui, Alex Tallant, Jon Boggia, and Priscilla Krai. Without a friendly working environment, research cannot be so joyful.

I am also grateful to Daniel Ragheb for his great ideas and help on thesis, my lovely friend, Titiyola Denyole for her sincere and trustful friendship and my coworker, Xinyi Huang, who provided valuable ideas during experiments and friendship during difficult times.

Last, but not least, my most sincere appreciation is to my parents, Fatma and Ibrahim Kocabas, for their unending love and support. It is the greatest fortune to be their beloved daughter.

CHAPTER ONE

INTRODUCTION

1.1 History of Tuberculosis

The disease Tuberculosis (TB), a current major cause of global death, has been observed in the world since ancient times as described by Hippocrates (400 B.C.) in his writing "Of the Epidemics."[1]. According to recent World Health Organization (WHO) studies, more than one-third of the world's population are infected with tubercle bacilli, the pathogen that causes TB [2]. In another word, 10 % of people infected with TB bacilli will be dangerously ill with active TB in their lifetime. Moreover, TB is a major cause of death among people who are HIV-positive [3].

Tuberculosis is caused by a group of closely related bacterial species termed the *Mycobacterium tuberculosis* complex (MTBC). Besides Mycobacterium tuberculosis; *Mycobacterium africanum, Mycobacterium bovis, Mycobacterium caprae, Mycobacterium microti,* and *Mycobacterium pinnipedii* are altogether referred to as the M. tuberculosis complex or tubercle bacilli [4].

The class to which these organisms belong is *Actinobacteria*, a large and diverse group of gram-positive bacteria with a high G/C nucleotide content in their DNA [5]. Furthermore, *Actinobacteria* are widely distributed in diverse ecosystems, such as soil and seawater [6], and are the cause of other significant human diseases, such as leprosy, and diphtheria [7].

As Sir John Crofton states, whose research revolutionized the treatment of tuberculosis, "the greatest disaster that can happen to a patient with TB is that the organisms become resistant to two or more of the standard drugs through selection of mycobacterial mutants that result from spontaneous chromosomal alterations." [8]. The fourth report on global anti-TB drug resistance, in 2008, shows the severity of the drug resistance problem in the world [9].

The increasing emergence of drug resistance and the problem of mycobacterial persistence highlight the need to develop novel TB drugs that are active against drug resistant bacteria but, more importantly, kill persistent bacteria and shorten the length of treatment. Recent new and exciting developments in tuberculosis drug discovery promise a possible revolution in the chemotherapy of tuberculosis. Although there is an urgent need to develop new TB drugs [10] in more than 40 years, not even a single

new drug has been developed and licensed for the treatment against TB (*e.g.* Rifampin, 1966) [11].

With some exceptions amongst the protozoa, aerobic and air-tolerant organisms produce low-molecular-mass thiols that are important for the maintenance of reducing intracellular milieu. For example, glutathione (GSH) is principal thiol in eukaryotes as well as cyanobacteria and proteobacteria to remove peroxides and generate a low level of reactive oxygen species [12,13]. One feature that is common to most of the members Actinobacteria is the production of mycothiol (MSH; also designated AcCys-GlcN-Ins), a small thiol that is often present in millimolar amounts and has analogous functions to glutathione (GSH), which is not found in *Actinobacteria* [12].

1.2 Discovery of Mycothiol (MSH) and Its Functions

Fahey and co-workers first noted but had not identified yet as mycothiol (MSH) in 1993, as the major low molecular weight thiol in cell extracts of streptomycetes, which were lacking in detectable levels of GSH. Researchers observed that an unknown thiol eluting at 17 minutes by HPLC analysis. At this point, its structure was not known and was referred to as U17 [14]. The following year Sakuda *et al,* isolated mycothiol disulfide

(MSSM) from *Streptomyces* sp. AJ9463 and suggested its structure based on NMR analysis and acid hydrolysis Three years later the discovery of MSH (1-*O*- (2-[*N*-acetyl-L-cysteinyl] amido-2-deoxy-α-D-glucopyranosyl)-D-*myo*-inositol), the same research group, Sakuda *et al* proposed a pathway for mycothiol biosynthesis [15].

Almost all of actinomycetes have been studied so far, which lack GSH show MSH as the major low molecular weight thiol [12, 14]. Based on our current information about MSH (in actinomycetes) and GSH metabolism (in GSH-utilising bacteria) [13,15], it appears that MSH serves as a functional alternative for GSH in the actinomycetes.

Besides its key role of glutathione in bacteria maintaining the proper oxidation state of protein thiols, glutathione also assists protecting the cell from the action of low pH, chlorine compounds, and oxidative and osmotic stresses [13]. Moreover, studies have demonstrated that mutants defective in glutathione biosynthesis show significantly increased sensitivity to oxidative stress and alkylating reagents [16].

Its known that mycothiol is the major thiol of the mycobacteria, its functions are analogous to those of GSH and also, enzymes involved in the metabolism of mycothiol could play a role in environmental adaptive

responses. The production and utilization of mycothiol are pathogen-specific processes that could be good drug targets [15]. Since the MSH pathway is not found in eukaryotes or other eubacteria, the enzymes involved in MSH biosynthesis present potential and specific chemotherapeutic targets for agents with activity against Actinomycetes, including mycobacteria.

Gene disruption studies have demonstrated that MSH plays a number of important protective roles in mycobacteria and is essential for growth and survival of *M. tuberculosis* [17, 18] on the contrary, this is not true of *M. smegmatis* [19]. Since *M. smegmatis* can survive and grow without MSH in addition to being non-pathogenic for humans, it is a useful model organism for studying mycothiol biosynthesis.

Although no survival mechanisms for *M. smegmatis* in absence of MSH have been identified, yet; most likely involve detoxification enzymes encoded in the larger genome of M. smegmatis (7 vs. 4.4 Mb) that are absent in M. tuberculosis [18]. Mutant strains of *M. smegmatis* with modifications, mutations, or deletions in the genes encoding a set of enzymes which involved in the biosynthesis pathway of MSH, MshA-D have been investigated for MSH production and drug susceptibility [19-22].

1. 3 Mycothiol Biosynthesis and Detoxification Pathway

The biosynthesis of MSH is a five-step process that involves four unique enzymes, MshA, MshA2, MshB, MshC, and MshD. The pathway for MSH biosynthesis originates with L-*myo*-inositol-1-phosphate, which is acquired from glucose-6-phosphate by the action of the inositol-1-phosphate synthase (Ino-1). Inositol-1-phosphate is then converted to MSH in five enzymatic steps (Figure 1.1)

The *N*-acetylglucosamine transferase (MshA) for 3-phospho-GlcNAc-Ins, which is subsequently dephosphorylated to generate 1-D-*myo*-inosityl-2-acetamido-2-deoxy-α-D-glucopyranoside (GlcNAc-Ins) by an unidentified phosphatase (MshA2) [23]. A metallo-protein *N*-Acetyl-1-D-*myo*-Inosityl-2-Amino-2-Deoxy-α-D-Glucopyranoside Deacetylase (MshB) deacetylates GlcNAc-Ins [24], and then MshC ligates Gln-Ins to l-cysteine [15]. MshD acetylates the Cys-Gln-Ins to form the final product, which is called MSH [25].

1.3.1 *N*-Acetyl-1-D-*myo*-Inosityl-2-Amino-2-Deoxy-α-D-Glucopyranoside Deacetylase (MshB)

The third enzyme in the MSH biosynthetic pathway is MshB that was identified in a genetic analysis of a selected MSH-deficient mutant strain of *M. smegmatis*. Although this strain cannot produce GlcNAc-Ins, it is able to utilize added GlcNAc-Ins from the medium for the synthesis of MSH [24]. The same study has demonstrated that the deacetylase activity of MshB and is encoded by the Rv1170 gene in *M. tuberculosis*.

The sequence of MshB is very similar to MCA which is an enzyme involved in electrophilic toxin elimination [26]. It has been shown that MCA has a low GlcNAc-Ins deacetylase activity that enables the production of MSH in the absence of MshB so that MshB is not essential for MSH synthesis or growth of *M. tuberculosis* [27]. One of the crystal structures of MshB from M. tuberculosis (in the absence of substrate) has showed that MshB is a zinc-dependent metallohydrolase [28,29]. Structural studies revealed that the N-terminal domain of MshB is similar to the fold of lactate dehydrogenase, with a zinc atom in the N-terminal domain, and is coordinated by His13, Asp16, His147 connected with two water molecules, one of which is most probably to leave upon the binding GlcNAc-Ins [28] (Figure 1.2). According

to the crystal structure with β-octylglucoside determined that the putative active site like a cavity closed in under C-terminal loops [29]. Furthermore, the mercuric acetate ion, which used in the structural determination, supported the possible positions of the Zn^{2+} ligands. One of the proposed catalytic mechanisms for MshB depends on the structural arrangement similarity of catalytic residues seen in metalloproteinases [28]. This mechanism suggests that the conserved Asp15 is the general base for water activation [28]. As shown in Figure 1.2, catalysis begins with the proton abstraction of the zinc-ligated water molecule by Asp15. The deprotonated water behaves as a nucleophile and attacks the amide carbonyl, which is polarized by the zinc. As a result, the tetrahedral transition state would be formed and stabilized by the positively charged Zn^{2+} and the side chain of His144, which connects to Asp146 by hydrogen bond. The carboxyl group of Asp15 serves as a general acid to transfer the proton to the amine, so that GlcN-Ins could release as product. However, we need detailed mechanistic studies to validate this hypothesis. The substrate specificity has been investigated for MshB and MCA and noticed that the overlap of substrate specificity for the two enzymes [30]. In this study, authors reported that MshB is a better deacetylase than MCA, except the monobimane derivative, CysmB-GlcNAc-Ins.

A study in 2007, MshB was screened with a library of natural bromotyrosine-derived compounds that were previously shown to inhibit MCA. Even though the inhibitory concentrations of the best candidates remain in the low micromolar range, further development and optimization of more potent inhibitors are needed [31].

1.3.2 Mycothiol-*S*-conjugate amidase (MCA)

Newton et al have mentioned "MSH *S*-conjugate amidase was accidentally discovered in our laboratory during an attempt to label MSH in *M. smegmatis* cells with mBBr before pelleting and extraction in order to ascertain whether the pelleting of cells influenced the MSH level."[26]. The bimane derivative of N-acetylcysteine (AcCySmB) is a compound that the member of a class known as mercapturic acids, final products excreted in urine of a GSH-dependent, multi-organ detoxification pathway in animals [32]. Although mercapturic acid production is a major detoxification pathway in mammals, GSH is the main source of the cysteine in the mercapturic acid pathway [33].

Actinomycetes are able to utilize a more efficient detoxification pathway through a single enzyme, mycothiol-*S*-conjugate amidase (MCA), which hydrolyses the glucosaminyl–amide bond of MS-conjugates to release the

mercapturic acid-labelled toxin and GlcN-Ins (Figure 1.3). Moreover, after the mercapturic acid derivatives are exported from the cell, the free GlcN-Ins is recycled back into the MSH biosynthetic pathway [26]. No mercapturic acid transporters have been identified so far [34].

In 2000, Newton et *al* successfully purified MCA from *M. smegmatis* and sequenced to identify the corresponding protein, encoded by Rv1082, in *M. tuberculosis* and they found that Rv1082 is 78% of identical in *M. smegmatis* MSMEG5261 [26]. We can state that similarities of MCA in MSH-producing bacteria suggest that MCA is important for MSH function. In addition, higher levels of sequence identity are detected for sequences of MCA orthologs from other mycobacteria, including *Mycobacterium bovis*, *Mycobacterium leprae*, and *Mycobacterium avium*. Moreover, the sequence of *M. tuberculosis* MshB (Rv1170) and MCA (Rv1082) are closely related homologues (42% identical) and MshB has amidase activity with mycothiol *S*-conjugates [35]. A similar study reported that homologues of MCA present in the antibiotic biosynthetic operons of other actinomycetes [12], the majority of which produce mycothiol [36]. In 2003, Sareen et al worked on the characterization of M. *tuberculosis* MCA. They successfully cloned and expressed the enzyme in *E. coli* for the purification and showed that it is

a zinc-containing enzyme that can be inactivated with the metal chelator 1,10-phenanthroline [17].

As mentioned earlier, MCA is able to *N*-deacetylate GlcNAc-Ins; that explains that in case of the redundancy of MshB, MCA provides the compensatory GlcNAc-Ins deacetylase activity that sustains 10% of the wild-type MSH levels in MshB null mutants [17]. In spite of this, MCA exhibits 4800-fold lower substrate efficiency (k_{cat}/K_m) for GlcNAc-Ins than MshB does. The homology model for the MCA active site which created based on the crystal structure of MshB shows perfect alignment of all the key active site residues with an exception of Lys-19 in the MCA model is in place of Ser-20 in MshB [28]. This may suggest that Ser-20 could play an important role in disaccharide binding and Lys-19 of MCA might prevent the ideal binding of GlcNAc-Ins for efficient catalytic turnover. Since MCA is able to recognize the same disaccharide motif, additional binding interactions between MCA and the CysNAc motif might promote a better binding of its mycothiol-*S*-conjugate substrates. The structural resolution of MCA would lead to reveal the relative substrate specificities for MCA and MshB so that potent dual MshB/MCA inhibitors can designed that would suppress MSH biosynthesis and MCA-mediated drug resistance, at the same time [37].

1.4 Research Objectives

Since the deacetylation reaction catalyzed by MshB is very similar to the cleavage of peptide bond by a protease, the active site of MshB is comparable to a metalloprotease. For example, the crystal structures of thermolysin and carboxypeptidase A show that these enzymes generally utilize a metal chelated by three protein ligands (usually two histidines and a glutamate). A general base carboxylate activates a water molecule to cleave the peptide bond. A nearly identical group of residues in the metalloprotease active site is observed in MshB deacetylase the ligands on the zinc are two histidines (His-13 and -147) and an aspartate (Asp-16), unlike the usual glutamate in the metalloproteases [28]. Maynes et al hypothesized zinc could be the active site metal based on metal analysis data showing Zn^{+2} in the active site, an X-ray fluorescence scan revealing the same, and the Zn coordination geometry that could be well accommodated in MshB and its homolog MCA [38].

In 2006, Newton et al reported that MshB contains a divalent transition metal ion that is essential for activity [30]. In the study, they inactivated MshB, isolated on the both Ni-affinity column and Zn-affinity resin by 1,10-phenanthroline, a potent metal chelator. They also observed that apo-MshB can be activated with Zn^{2+}, Ni^{2+}, Mn^{2+}, or Co^{2+}, the last providing the highest

activity, a feature common to many metallopeptidases [39]. Although, a range of transition metals can activate MshB, Zn^{2+} is the metal found in MCA, a homolog of MshB, when isolated without the use of a metal-affinity column under aerobic conditions [35] so, it is presumed that Zn^{2+} is present in native MshB [30]. The results from the phenanthroline inhibition experiments suggest that a divalent metal is required for activity of MshB and most likely its homologous MCA. In addition, the metal binding ligands determined by X-ray crystallography of MshB [28] can be seen in the MCA sequences of diverse gram-positive bacteria [29]. Extensive studies on identifying inhibitors of MCA include oxime and other potential metal binding moieties [40, 41].

It is essential to know the native cofactor of a metalloenzyme, in order to design the most effective inhibitor. Recent studies have re-classified several "Zn^{2+}-dependent" enzymes as "Fe^{2+}-dependent" enzymes, including peptide deformylase (PDF) [42,43,44], LuxS [45] and possibly histone deacetylase 8 (HDAC8) [46]. As mentioned earlier, a range of transition metals can activate MshB. However, in the studies the ability of Fe^{2+} to activate MshB was not examined. It has been theorized upon rapid oxidation of Fe^{2+} to Fe^{3+} it can be replaced by Zn^{2+} in the active site; as a result, the native metal

cofactor of aerobically purified enzymes could be misidentified as Zn^{2+} [47]. For example, at first, LpxC was classified as a "Zn^{2+}-dependent" deacetylase based on the observations that LpxC activity is reversibly inhibited by with metal chelators [e.g., ethylenediaminetetraacetic acid (EDTA) and dipicolinic acid (DPA)] and LpxC is co-purified with Zn^{2+} under aerobic conditions [48]. One of the following studies has demonstrated that under normal growth conditions the native metal is Fe^{2+} in the active site of LpxC in *E. coli* [47]. In the same study, authors state that "it is possible that the active site metal bound to LpxC in vivo could switch depending on the metal ion availability, thus allowing LpxC to function using different metal ion cofactors under different environmental conditions."

Mycobacterial enzymes MshB and MCA may use the metal ion, which is abundant in the environment under aerobic conditions. Furthermore, another possibility is that the enzymes use multiple cofactors and change them according to their physiological needs under different environmental conditions. We are interested in further understanding the potential reasons a metalloenzyme would choose one metal ion over another. This would allow us to understand the basics of biological regulation of enzyme function and the roles of these metal ions.

In our study, we aim to biochemically characterize recombinant MshB and MCA from *M. smegmatis (Ms)* and *M. tuberculosis (Mt)* by determining the respective enzymes' cofactor. We worked on identifying the native metal ion cofactor(s) of the enzymes, and specifically examining possible environmental conditions such as metal ion availability and affinity. To reach our goal, we performed pull-down experiments with N-terminal HaloTag® fused recombinant proteins, *Mt/Ms* MshB and *Mt/Ms* MCA, under different environmental conditions such as expressing MshB and MCA in either LB media, or CDM (chemically defined media) supplemented with Zn, Fe, or no metal ions. We also performed pull-down experiments under aerobic and anaerobic conditions. These data were supported with the metal binding affinities of MshB and MCA.

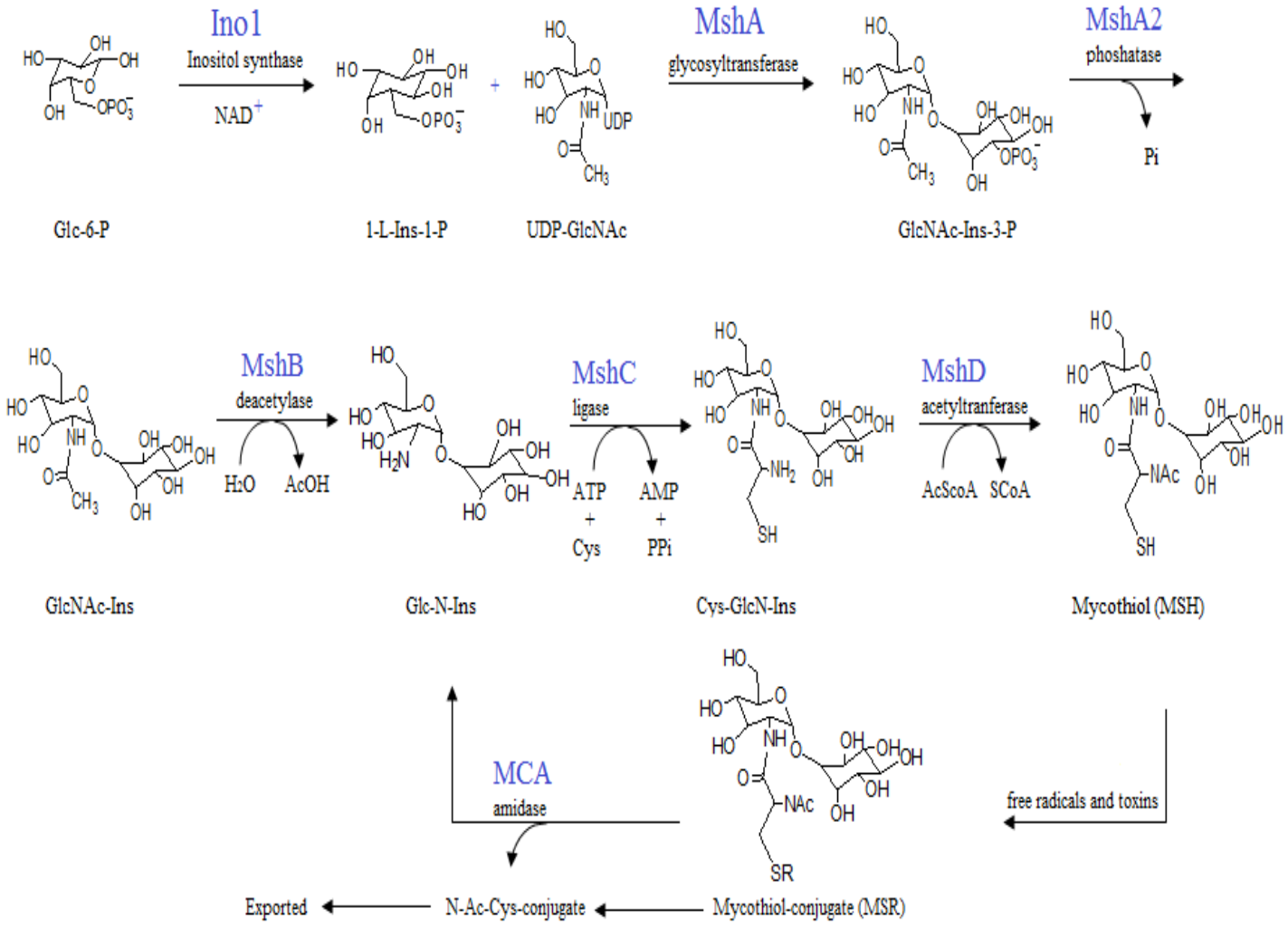

Figure 1.1. The Biosynthesis and Detoxification Pathway of Mycothiol

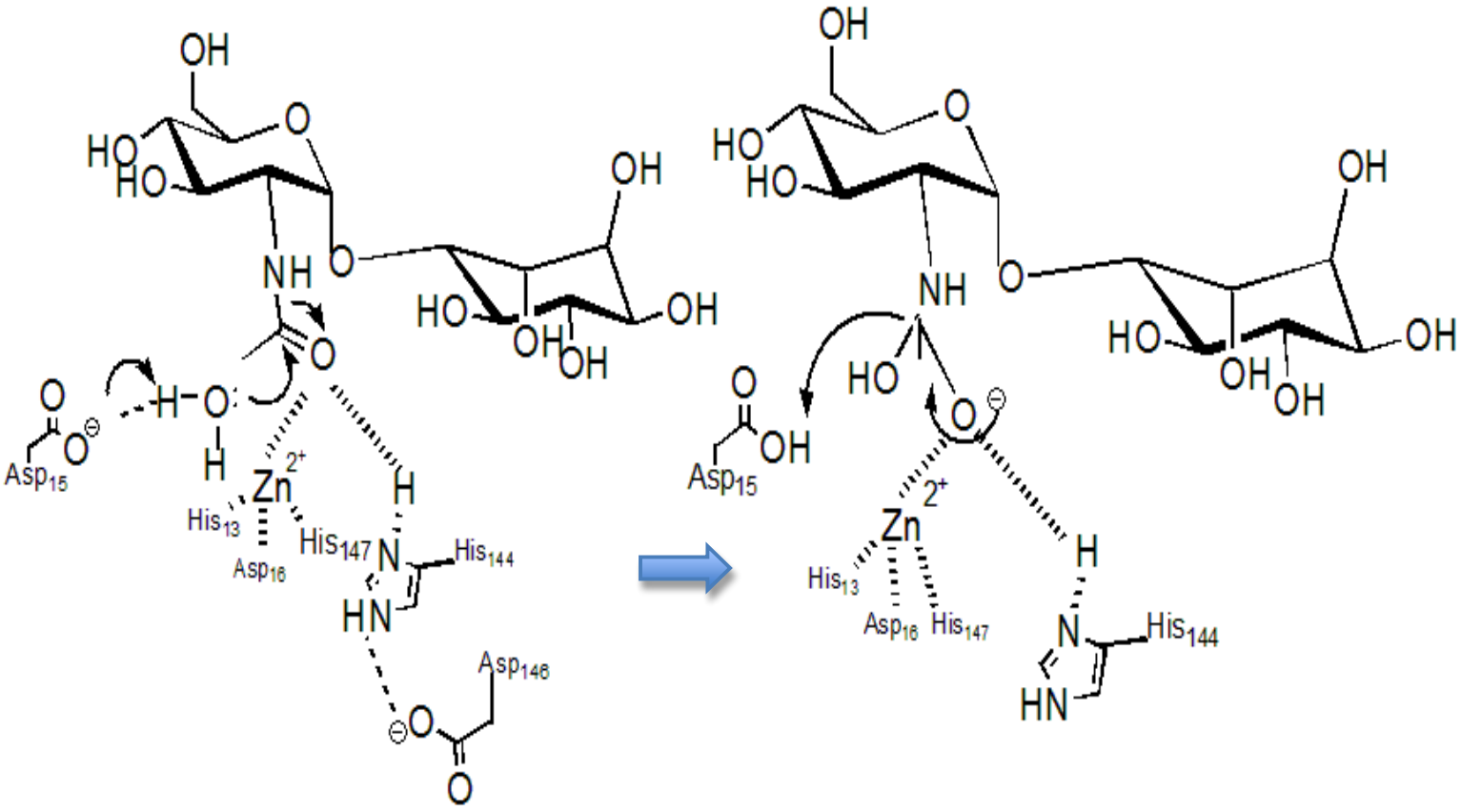

Figure 1.2. A purposed catalytic mechanism for MshB. In this mechanism, the conserved Asp15 serves as general base and deprotonates water molecule in the active site, which performs a nucleophilic attack to the amide carbonyl polarized by the zinc atom.

CHAPTER TWO

PULL-DOWN EXPERIMENTS WITH HALO- MshB AND MCA

I. Introduction

The full pathway of MSH biosynthesis and detoxification includes various promising drug targets. In this study, we focused on the biochemical characterization of two recombinant metalloenzymes, MshB and MCA, from *M. smegmatis and M. tuberculosis*. Knowing the native cofactor(s) of the target enzymes is essential to develop inhibitors as drugs, as inhibitors of metalloenzymes typically contain a metal-binding group that binds to the active site metal ion. Previous studies have showed that divalent metals activate MshB and MCA. However, in these studies the ability of Fe^{2+} to activate MshB was not examined. In the Hernick laboratory, it has been revealed that Fe^{2+} bound MshB exhibits higher activity than when it is bound Zn^{2+}-MshB (X. Huang and M. Hernick, unpublished results). Moreover, the presence of oxygen causes that Fe^{2+} bound MshB loses its activity in the length of time (X. Huang and M. Hernick, unpublished results). Recently, several "Zn^{2+}-dependent" enzymes have been re-classified several as "Fe^{2+}-dependent" enzymes, including peptide deformylase (PDF) [42,43,44], LuxS [45], and possibly histone deacetylase 8 (HDAC8) [46]. LpxC is also one of

the re-classified enzymes that co-purifies Fe^{2+} under anaerobic conditions [68] and shows higher activity when it employs Fe^{2+} as co-factor [47].

In light of these observations, we aimed to examine possible native metal ion cofactor(s) used by MshB and MCA under different environmental conditions, such as metal ion and/or oxygen availability. MshB and MCA were generated as fusion proteins with a N-terminal HaloTag®. These recombinant proteins expressed in chemically defined medium supplemented with iron, zinc, or both, in *E.coli* and purified under aerobic and anaerobic conditions.

II. Materials and Methods

2.2.1 Materials

Primers were designed and purchased from Integrated DNA Technologies. Enzymes used for cloning were from New England BioLabs, Epicenter and Promega Corporation (Madison, WI). *E. coli* SMART CELL and BL21(DE3)^{R} chemically competent cells were from Genelantis and Invitrogen , respectively. The pFN18K HaloTag® T7 Flexi® Vector was used for constructing halo-MshB and halo-MCA. DNA sequencing was performed at the Virginia Bioinformatics Institute DNA Sequencing Facility (VBI). Protein purifications performed with HaloLink^{TM} (Promega) Resin.

All chemicals used in buffers were purchased from Thermo,Fisher Scientific and Sigma-Aldrich.

During the purification process, all solutions were prepared in "metal-free" plastic ware, with reagents that did not contain extraneous metal ions and/or were treated with Chelex (Biorad). MilliQ water was used in solutions in the experiments with an 18.2 μΩ resistance. The metal content of solutions, reagents and proteins were measured by ion chromatography (ICS-3000) (Dionex).

2.2.2 Cloning of N-terminal HaloTag® fused MshB and MCA

The HaloTag® (Promega) is a 34kDa mutated hydrolase and it covalently binds to HaloLink™ Resin via an immobilized chloroalkane ligand [59]. TEV Protease cleaves the target protein from the resin. The TEV Protease cleaved purified protein can be recovered. pFN18K HaloTag® T7 Flexi® Vector that encodes the HaloTag® protein and expresses protein in *E. coli* (Figure 3.1) [59]. Like other Flexi® cloning systems (Promega), the vector for HaloTag purification system has two rare restriction enzyme recognizing sites, SgfI at the 5' end and PmeI at the 3' end. We obtained encoding sequences for MshB and MCA from another Flexi® Vector, the pVP56K plasmid, which was inserted MshB and MCA genes described previously,

were digested with Flexi® enzyme blend and then, interested genes were gel extracted by using The Wizard® SV Gel and PCR Clean-Up System (Promega). We cloned *Mt/Ms* MshB and *Mt/Ms* MCA genes into pFN18K HaloTag® T7 Flexi® Vector. Generated plasmids were transformed in BL21(DE3)® *E.coli* cell line further protein purification.

The expression of halo-tagged recombinant proteins, *Mt/Ms* MshB and *Mt/Ms* MCA, were examined by SDS gel. Fusion *Mt/Ms* MshB and *Mt/Ms* MCA were expressed in both Luria-Bertani Medium (LB) (Fisher Scientific) and chemically defined medium (CDM), prepared as previously described [60].

One of the advantages of pull-down protein purification method is to let us to use less amount of cell culture such as 50 or 100 ml. Moreover, by using this method we were able to complete the purification of MshB and MCA in an anaerobic chamber that provides us under anaerobic conditions for protein purification. Thus, we are able to show Fe(II) existence in the protein by avoiding the unstable, oxidized state, Fe(III), of iron.

2.2.3 Expression, Rapid Purification with HaloLink® Resin and TEV Protease Cleavage

E. coli BL21(DE3) cells transformed with N-terminal halo-MshB and halo-MCA were grown in Chemically Defined Medium (CDM). Chemically defined medium is composed of a medium (7.6 mM $(NH_4)_2SO_4$, 33 mM KH_2PO_4, 60 mMK_2HPO_4, and 1.7 mM sodium citrate) supplemented with 40 μg/ml of all 20 essential L-amino acids (Sigma), 0.2% glucose, 1 mM$MgSO_4$, and 5×10^{-5}% thiamine. Well-dissolved solution except thiamine and $MgSO_4$ was incubated overnight with 50 g/liter Chelex 100 resin (Bio-Rad) to eliminate trace metals, sterile-filtered and aliquoted in metal-free tubes before use [60]. Protein expression was induced when the cells reached an OD_{620} of 0.6 by the addition of 1 mM isopropyl-*β*-D-thiogalactoside (IPTG) along with the addition of either no added metals, 20 μM $ZnSO_4$, 20 μM ferric ammonium citrate, or both metal supplements and the cells were incubated overnight at 25 °C. The cells were harvested by centrifugation, washed once with 5 mM $CaCl_2$ and twice with 10 mM Mops pH 7. The washed cell pellets from 50 or 100 mL growth medium were transferred to an anaerobic glove box, resuspended in 3 mL pull-down buffer (40 mM Mops, 150 mM NaCl, 10 mM tris (2-carboxyethyl) phosphine (TCEP), pH 7.5) and lysed by incubation with lysozyme (1 mg/mL) at room

temperature for 15-30 minutes. The cell lysate was cleared by centrifugation (15, 000 rpm, 25-30 min.) either in an anaerobic glove box or on the bench. A small amount of cleared lysate (100 µL) was reserved for IC analysis, and the rest of cleared lysate was incubated with, previously equilibrated with the pull-down buffer, 150 µL HaloLink^{TM} Resin for 30 minutes. The HaloLink^{TM} Resin was washed with 5 x 500 µL pull-down buffer, resuspended in 250 µL pull-down buffer, which contains TEV protease (5 U/µL) at 37°C for 45-60 minutes. TEV protease, used in pull-down experiments, was expressed and purified in our laboratory with an insignificant amount of metal content (<0.001 metal ion per protein). Resin and cleaved proteins were separated by centrifugation (13.2 rpm, 2 min) for the further analysis of the metal content of the purified protein by IC. Metal content analyses were completed by determination of MshB or MCA in the eluate by the Bradford Assay (Sigma) with BSA (Sigma) as the standard.

III. RESULTS

2.3.1 Cloning of N-terminal HaloTag® fused MshB and MCA

We have cloned *Mt/Ms* MshB and *Mt/Ms* MCA genes which have SgfI at the 5' end and PmeI at the 3' end into pFN18K HaloTag® T7 Flexi® Vector. We observed high expression levels of halo-tagged recombinant proteins, *Mt/Ms* MshB and Ms/*Mt* MCA in both LB supplemented with 100 μM zinc final concentration and CDM supplemented with 20 μM iron, zinc or both. Moreover, expected size proteins were soluble and were verified by 12% SDS-PAGE gel (RunBlue) (Figure 2.2).

2.3.2 Expression, Rapid Purification with HaloLink™ Resin and TEV Protease Cleavage of MshB and MCA

We purified halo-MshB and MCA from *Mycobacterium tuberculosis* and *Mycobacterium smegmatis* under aerobic and anaerobic conditions to clarify the identity of the biologically relevant metal ion cofactor using HaloLink™ Resin system.

We carried out pull-down experiments aerobically on the bench-top or anaerobically in an anaerobic glove box. Our aerobic pull-down experiments supported the observation from previous studies on the characterization of MshB and MCA that is these enzymes bind Zn (II) after aerobic

purifications [28, 29]. We determined that *Mt/Ms* MshB and *Mt/Ms* MCA co-purify with either Zn (II) or Fe(II) under aerobic conditions (Figure 2.2).

It is known that Fe(II) can rapidly oxidize and loses its atomic stability. As a result, Fe(III) could leave the active site of the enzyme and be replaced with a more oxidation-resistant divalent metal ion such as Zn(II) or Ni(II). We performed a series of pull-down experiments in the anaerobic glove box to test the existence of Fe(II) . We observed that *Mt/Ms* MshB and *Mt/Ms* MCA co-purify with mostly Fe(II) and less Zn(II) under anaerobic conditions compare to results from aerobic pull-down experiments whereas no other divalent metal ions (e.g. Co, Ni, Cu) are observed at greater than trace levels (<3 - 5%) (Figure 2.3). It is possible that MshB and MCA from *Mycobacterium tuberculosis* and *Mycobacterium smegmatis* could prefer Fe(II) as co-factor *in vivo* . These enzymes purified from cells grown in minimal (CDM) medium with or without iron supplementation contains mainly bound Fe(II) (Figure 2.3); however, supplementation of the medium with zinc increases the Zn bound to halo-MshB and halo-MCA.

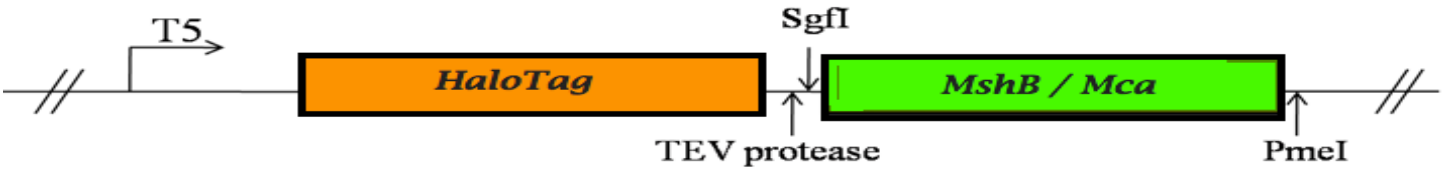

Figure 3.1. Schematic of the pFN18K HaloTag® T7 Flexi® expression vector

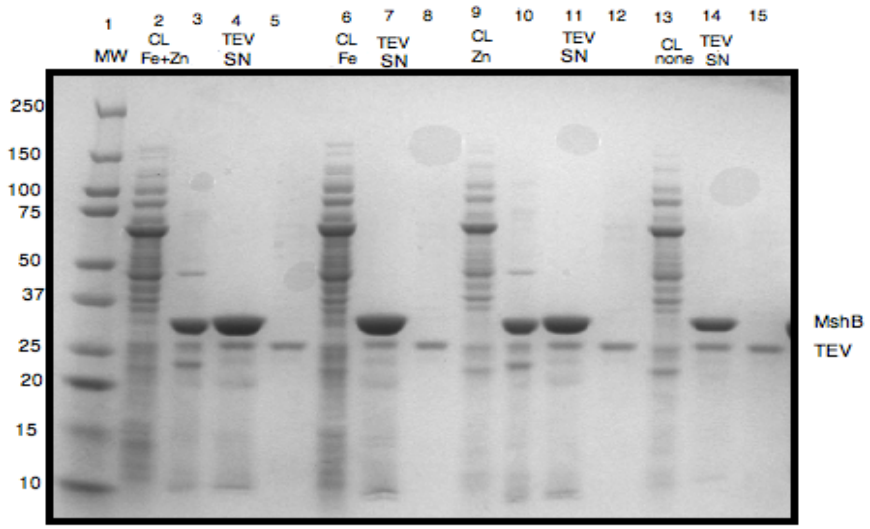

Figure 3.2. Pull-down experiment of *Ms* MshB. Halo-*Ms* MshB was expressed in BL21(DE3) *E. coli* grown in minimal medium with and without Fe or Zn supplementation (5 – 20 μM) and induced overnight at 20°C by addition of 1 mM IPTG. The protein was purified using halo resin under anaerobic conditions as described Section 2.2.3.

1. Protein marker (Kaleidoscop)®
2. Clear cell lysate of *Ms* MshB (Both CDM) (1:1 diluted)
3. MshB as control
4. TEV cleaved *Ms* MshB (Both-CDM)
5. TEV as control
6. Clear cell lysate of *Ms* MshB (Fe- CDM)(1:1 diluted)
7. TEV cleaved *Ms* MshB (Fe-CDM)
8. TEV as control
9. Clear cell lysate of *Ms* MshB (Zn-CDM)(1:1 diluted)
10. MshB as control
11. TEV cleaved *Ms* MshB (Zn-CDM)
12. TEV as control
13. Clear cell lysate of *Ms* MshB (None- CDM)(1:1 diluted)
14. TEV cleaved *Ms* MshB (None- CDM)
15. TEV as control

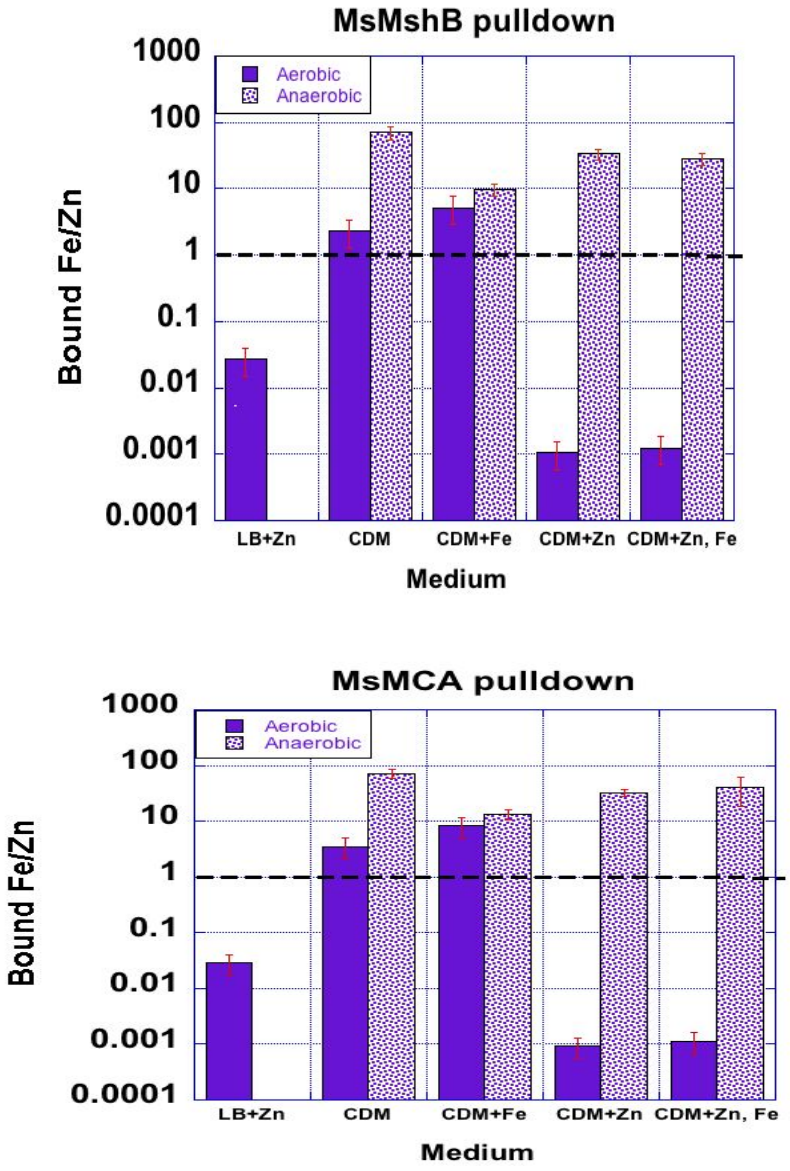

Figure 2.3. Comparison of metal content of MshB and MCA were isolated from *E. coli* aerobically and anaerobically. Halo-MshB and halo-MCA was expressed in BL21(DE3) *E. coli* grown in minimal medium with and without Fe or Zn supplementation (20 μM) and LB Medium induced by addition of 1 mM IPTG . The protein was purified using a halo resin protein purification method under anaerobic and aerobic conditions (see Section 2.2.3). TEV cleaved protein was analyzed by IC. Data correspond to the average and standard deviation from 3 replicate experiments.

IV.DISCUSSION

2.4.1 Cloning of N-terminal HaloTag® fused MshB and MCA

We have also cloned *Mt/Ms* MshB and *Mt/Ms* MCA genes into pFN18K HaloTag® T7 Flexi® Vector. This technique significantly reduces errors during the cloning experiments. We obtained high levels of expression of halo-MshB and MCA recombinant proteins with this cloning strategy.

Halotagged MshB and MCA were expressed in both Luria-Bertani Medium (LB) and CDM supplemented with 100μM final concentration of zinc, 20μM final concentration of iron, zinc or both. We employed these different growth conditions to provide distinct environmental conditions for MshB and MCA to perceive possible effects of metal ion availability on their co-factor preferences. The expression levels of LB growth proteins are slightly higher than the expression levels of CDM growth media (data not shown). Results from these experiments indicate that MshB and MCA purified from cells grown in minimal (CDM) medium with iron supplementation contains mainly bound Fe (Table 3.2); however, supplementation of the medium with only zinc increases the Zn bound to MshB and MCA.

2.4.2 Expression, Rapid Purification with HaloLink® Resin and TEV Protease Cleavage

In order to determine the native metal ion cofactor of an enzyme, certain factors in the experimental procedures for protein expression and purification need to be taken into consideration. First, the affinity tag fused to the recombinant proteins should not bind any metal ion naturally. Second, it is necessary for the purification process to be rapid with the minimal number of steps to avoid any possible metal-switching occurrence and minimize possible external metal contamination during the purification steps. Another important feature is the method should be suitable for a small-scale purification so that we can perform pull-down experiments in anaerobic chamber.

The HaloTag® Protein Purification System is based on a unique tag, the HaloTag® protein, which is a mutated hydrolase, so that the proteins can be expressed in *E. coli* as N-terminal HaloTag® fusion proteins (Figure 3.2). The HaloLink™ Resin provides a method for covalent attachment of HaloTag® fusion proteins. The resin consists of a HaloTag® ligand bound to Sepharose® beads that specifically (covalent) and rapidly binds to the HaloTag® fusion proteins [61].

Another important point to notice is the amount of TEV protease used to cleave the interested enzyme from halo-tag bound resin. In order to determine the minimal and functional amount of TEV, we performed a series of pull-down experiments with different concentrations of the protease, incubation times and temperatures. From these experiments, we were able to determine the best TEV cleavage conditions for pull-down experiments (list what these are). We are able to complete all protein purification process in three to four hours.

2.4.3 Results from Pull-down experiments

A recent study showed that in the presence of oxygen, the Fe(II) cofactor bound to LpxC is oxidized to Fe(III) which dissociates and is replaced by Zn(II) [47]. MshB purified from *E. coli* was previously shown to contain bound Zn(II); however, this protein was purified under aerobic conditions using Zn-affinity resin [28]. Our laboratory has observed that apo-MshB shows higher enzymatic activity after incubation with appropriate Fe(II) buffer than incubation with Zn(II) buffer (X. Huang and M. Hernick, unpublished results), leading us to probe whether Fe(II) may serve as a cofactor for MshB and MCA. In order to examine the *in vivo* metal content of MshB and MCA, while avoiding possible oxidation of Fe(II), we purified HaloTag fused *Mt/Ms* MshB and *Mt/Ms* MCA under anaerobic conditions

by a rapid purification method, pull-down experiment. After TEV cleavage, the concentrations of metals and protein of the purified proteins were determined by IC and Bradford assays, respectively.

Results from these pull-down experiments reveal that MshB and MCA from *Mycobacterium tuberculosis* and *Mycobacterium smegmatis* purified from *E. coli* contain mainly bound Fe(II) under anaerobic conditions. These enzymes purified from cells grown in minimal (CDM) medium with iron supplementation contains mainly bound Fe (II) (Table 3.2); however, supplementation of the medium with only zinc increases the Zn bound to halo-MshB and halo-MCA under aerobic conditions. This may suggest that MshB and MCA from *Mycobacterium tuberculosis* and *Mycobacterium smegmatis* may prefer Fe(II) as their co-factor under anaerobic conditions, while under aerobic conditions either Fe(II) or Zn(II) serves as the cofactor depending on metal ion availability. It is possible that these enzymes may use multiple co-factors by a metal-switching mechanism to adapt to changing environmental conditions and/or regulates activity.

CHAPTER THREE

MYCOBACTERIAL MshB AND MCA METAL ION AFFINITY MEASUREMENTS

I. Introduction

The results from the pull-down experiments with MshB and MCA described in Chapter 2 indicate that these enzymes co-purify with Fe(II) under anaerobic conditions, and Zn(II) or Fe(II) under aerobic conditions depending on metal availability. In order to have a further insight into these results it is important to determine the iron and zinc affinities for these enzymes to clarify the possible reasons that enzymes prefer to be bound iron or zinc. It is possible is that after anaerobic purifications, we observed Fe(II) bound to these enzymes because Fe(II) has a higher affinity for the enzymes than Zn(II) has and Fe (II) is readily available in the cell.

Therefore, we aimed to determine the MshB and MCA affinity for Zn(II) and Fe(II) and compare these values to known concentrations of metal ions to determine if cofactor preferences are based solely on metal ion affinity/availability. Iron and zinc are present in high concentrations (close to 200 μM) in *E. coli* however, the concentrations of "free" metal ions can vary widely [49]. The estimated concentrations of total Zn^{2+} and Fe^{2+} per

Mycobacterium tuberculosis cell are comparable to that observed in *E. coli*, and are approximately 37.8±25.2 μM, and 505 ±215μM, respectively [49,50].

We determined the Zn(II) and Fe(II) dissociation constant (K_D^{metal}) values for recombinant MshB and MCA from *Mycobacterium tuberculosis* and the commonly used model species, non-pathogenic *M. smegmatis*. Results from these experiments indicate that MshB and MCA affinity for Zn(II) to be in the picomolar range and Ms MshB affinity for Fe(II) in nM range. These results suggest that the cofactor bound to MshB and MCA under anaerobic conditions is independent to their affinities for these metal ions.

II. Materials and Methods

3.2.1 Materials

Primers were designed and purchased from Integrated DNA Technologies. Enzymes used for cloning were from New England Biolabs, Epicenter and Promega Corporation (Madison, WI). *E. coli* SMART CELL and BL21(DE3)^R chemically competent cells were from Genelantis and Invitrogen , respectively. The pVP55A and pVP56K plasmids were obtained from Dr. Pablo Sobrado. DNA sequencing was performed at the Virginia

Bioinformatics Institute DNA Sequencing Facility (VBI). We used Ni-affinity chelating sepharose for the protein purification. All chemicals used in buffers were purchased from ThermoFisher Scientific and Sigma-Aldrich.

In metal-affinity assays, all solutions were prepared in "metal-free" plastic ware, with reagents that did not contain extraneous metal ions and/or were treated with Chelex (Biorad). MilliQ water with a resistivity of 18.2 MΩ was used for all solutions. The metal content of solutions, reagents and proteins were measured by ion chromatography (IC-3000) (Dionex).

3.2.2 Mutation and Cloning of *Mt* MshB in pVP56K and pVP55A

The Flexi® cloning system is a very effective directional cloning method for protein-coding sequences. The cloning system contains SgfI and PmeI, which are two rare-cutting restriction enzymes. The restriction sites for enzymes were introduced at the ends of the protein-coding region of interest. Then, the protein-coding region for *Mt* MshB was amplified from *Mycobacterium sp*. BCG by using two primers, one containing an SgfI site, the other containing a PmeI site. As a result, PCR products MshB of *M. tuberculosis* have the flanked restriction cut site of SgfI at the 5' end and PmeI at the 3' end.

Mt MshB encoding region has an internal SgfI restriction enzyme cutting side between 150 -156 nucleotides at the 5' end. In order to remove this enzyme site from *Mt* MshB gene, we mutated 153T to C, which causes a silent mutation in the gene. The PCR product of *Mt* MshB from *Mycobacterium sp*. BCG was inserted into a blunt-end cloning vector obtained from StrataClone™ Blunt PCR Cloning Kit (Stratagene) and ligation mixture transformed into StrataClone™ SoloPack® Competent Cells (Stratagene). After the isolation of plasmids with Wizard® Plus SV Minipreps DNA Purification System, we used a QuikChange Site-Directed Mutagenesis Kit (Stratagene) to mutate the thymine 153 to cytosine, using the appropriate primers in a single step PCR amplification. After eliminating the parent strands used as template during PCR reaction, we purified the reaction mixture with Wizard® SV Gel and PCR Clean-Up System (Promega).

Both PCR products and the plasmids, pVP55A and pVP56K, were digested with Flexi® enzyme blend (SgfI and PmeI) . The amplified gene was ligated into digested pVP55A and pVP56K expression plasmids to generate His8-*Mt* MshB and His8-MBP- *Mt* MshB constructs, respectively (Figure 3.1). The ligation mixture, pVP56K or pVP55A containing the interested genes, was directly transformed into *E. coli* (SmartCells) for over night incubation

with antibiotic contained agar plates at 37 °C . The pVP55A and pVP56K plasmids have resistance genes for antibiotics, which are ampicillin and kanamycin respectively, that allow us to screen MshB and MCA inserted plasmids on appropriate antibiotic contained Luria-Burtani (LB) broth agar plates. The affinity tags on the enzymes were attached by a sequence of amino acids that corresponded to a specific cleavage site for the Tobacco Etch Virus (TEV) protease to allow for tag removal during the purification process. Single colonies were selected and grown 10 ml LB contained either ampicillin or kanamycin at 37 C° in the shaker (225 rpm). After 12 hours, plasmids were isolated using Wizard® Plus SV Minipreps (Promega). DNA sequencing confirmed the presence of the desired genes. The His8-MBP-*Mt/Ms* MCA and His8-MBP- *Ms* MshB constructs were generated in our laboratory, previously (H. Liu and M. Hernick, unpublished results).

3.2.3 Expression, Purification and Preparation of Apo- *Mt* MshB

The pVP56K: *Mt* MshB expression plasmid expresses *Mt* MshB as a fusion to maltose binding protein (MBP) and His-tag. First, a culture (250 ml) of BL21(DE3)^{R} cells containing the pVP56K: *Mt* MshB plasmid was grown to inoculate two 2-L flasks of Luria-Burtani (LB) broth supplemented with kanamycin (50 μg/ml). Cultures were grown with shaking at 225 rpm at 37^{o}

C. Once cultures reached to an OD_{600} ~ 0.6, they were induced by adding 1 mM isopropyl-β-D-1-thiogalactopyranoside (IPTG). After overnight of induction at 25^{o} C, cells were harvested by centrifugation and stored at -80^{o}C. Cell pellets were resuspended in Buffer A (30 mM HEPES, 150 mM NaCl, 0.5 mM imidazole, pH 7.5). Cells were homogenized by high-pressure homogenizer (EmulsiFlex-C3, Canada), and then the lysate was clarified by centrifugation (18,000 rpm for 60 min). The cleared lysate was loaded onto an Immobilized Metal-Affinity Chromatography (IMAC) column previously charged with 0.2 M nickel chloride solution and equilibrated with buffer A (Ni-IMAC). The column was washed with Buffer A, Buffer A + 10 mM imidazole, Buffer A + 25 mM imidazole and *Mt* MshB was eluted with a 250 mL Buffer A + 250 mM imidazole in a fraction collector (Model 2110, Bio Rad) at a volume of 6 ml per tube.

Fractions containing His_8-MBP- *Mt* MshB were identified using SDS-PAGE, combined and concentrated by centrifugation to a 50 mL volume using Amicon MWCO 10K ultrafiltration devices (Millipore). After the transfer of the concentrated solution of His_8-MBP- *Mt* MshB into Slide-A-Lyzer Dialysis Cassettes (10K MWCO) (Thermo Scientific), *Mt* MshB was cleaved from the His_8-MBP tag by the addition of tobacco etch virus (TEV)

protease (300 μg/ml, 6.08 mg/ml) with an overnight cleavage in the dialysis buffer (30 mM Hepes, 150 mM NaCl, 1 mM TCEP) at 4^{o} C.
Following the incubation, to separate the cleaved protein from the removed tags, TEV protease, (which has a His-tag) and uncleaved protein, the mixture was run over the Ni-IMAC column, which was equilibrated with buffer A, and eluate was collected in a fraction collector at a volume of 6 ml per tube. After the determination of fraction tubes, which contained cleaved *Mt* MshB solution with SDS-PAGE, they were concentrated with MWCO 10K filters (Millipore) and protein concentrations were measured by Bradford assay by using as bovine serum albumin standard (ThermoScientific).

To remove metals from the metallo-enzyme, we incubated *Mt* MshB (final concentration 100 μM) with a buffer contains chelating agents (20 mM DPA, 10 mM Hepes, 250 μM EDTA pH: 7.6) for 45 min on ice. Then the solution was passed through an Econo-Pac 10-DG desalting column (Bio-Rad). We eluted the protein with gel filtration column buffer (25 mM Hepes, 1.5 mM TCEP, pH: 7.5) after the concentration of the eluted solution; Bradford assay and IC measurements were performed to determine final protein concentration and total metal content, respectively (Table 3.1). In order to avoid any metal contamination, we treated all solutions with

Chelex-100 resin (Bio-Rad) and verified them with IC analysis. Apo enzymes, which are used for the zinc affinity measurements of *Ms* MshB and *Mt/* Ms MCA, were expressed, purified and prepared, previously (H. Liu, P. Krai and M. Hernick, unpublished results).

3.2.4 Zinc affinity determination by ultra-filtration binding

We incubated Ultra-filtration devices (Microcon MWCO 30K) with 10 mM HEPES pH 7.5, 500 μM EDTA, 100 mM dipicolinic acid (DPA) for 30 minutes (500 μL), followed by 3 x 500 μL washes with ultrapure water to eliminate any extraneous metal ions. Commercial zinc standard (1000 mg/L) (TraceCERT®, Sigma Aldrich) was diluted in a pH buffer containing 1 mM nitriloacetic acid (NTA), 5 mM Mops pH 7 [51]. A set of various concentrations of Zn^{+2}_{total} (0 – 3.3 nM Zn_{free}) metal buffers, which are the range in 10^{-9} and $9.6x10^{-4}$ M, were prepared (Table 3.3). The concentration of Zn_{free} in the metal buffers was calculated using the program MINEQL+ (Environmental Research Software) [52].

We performed a number of affinity assays with four sets of apo-proteins (*Mt/Ms* MshB, and *Mt/Ms* MCA) that were incubated with various concentrations of Zn buffers for ≥25 minutes in 1 mM Nitrilotroacetic acid (NTA) and 5 mM Mops, pH 7.0 at room temperature. The free and bound

metal ions were separated by centrifugation (1500 x rcf, 5 min) in an ultra-filtration device. After that, the metals in an equal volume (50,75 or 100 µL of filtrate and retentate were analyzed by ion chromatography (IC-3000, Dionex). In the reaction at the equilibrium, the filtrate and retentate represent the amount of unbound zinc and the total product, which is zinc bound enzyme and unbound zinc, respectively. The $E \cdot Zn/E_{total}$ ratio was determined as a function of E_{total}. The concentration of Zn_{free} in the metal buffers was calculated using the program MINEQL+ (Environmental Research Software). Results from IC were analyzed and plots were obtained using the programs KaleidaGraph (Synergy Software, Reading, PA) and Wolfram Mathematica (Wolfram Research, Inc., Champaign, IL).

The value of K_D^{Zn} was obtained by fitting equation (1) [52].

Equation (1):

$$\frac{E \cdot Zn}{E_{tot}} = \frac{A_{endp}}{1 + \frac{K_D}{Zn_{free}}} + 1P$$

Where $E \cdot Zn$ is the concentration of Zn bound enzyme, E_{total} is the concentration of enzyme, K_D is dissociation constant and Zn_{free} is the total amount of free Zn.

3.2.5 Iron affinity determination by activity assay

Based on a recent published study, we decided to measure the affinity of MshB for Fe(II) determining from enhancement of catalytic activity [52]. The activity of enzyme was measured in the presence of various free Fe(II) concentrations, as calculated by MINEQL+ (Environmental Research Software), in an anaerobic glove box in 1 mM NTA (Nitrilotriacetic acid), 5 mM Mops (3-morpholinopropane-1-sulfonic acid) pH 7. Apo-*Ms* MshB, final concentration is 1µM in 200 µl total reaction volume, was incubated with the solutions which have the concentration range of 0 – 950 µM total Fe ($Fe(II)_{free}$ 0-2.6 µM) on ice for 30 min in the anaerobic glove box (Table 3.2). After the mix of the 20µl reaction buffer (50mM Hepes, 50 mM NaCl at pH: 7.5), the reactions were initiated 20 µl N-acetyl-D-glucoseamine (20 µl) as substrate at a final concentration of 50mM at 30°C. The enzymatic reactions (30µl) were stopped at six different time points (0,3,6,9,12,15 minutes) by adding (10 µl) 20% trichloroacetic acid (Fisher). Following to the stopping enzymatic reaction, 75µL 1M Borate buffer (pH: 9) was added to 25µL reaction mix in the 96 UV well plates. Before read the fluorescence intensity, 30µL Fluorescamine (2mg/mL) was added to the reaction mixture.

Fluorescamine is a fluorogenic reagent that is not fluorescent itself, but is able to form fluorescent products by reacting with primary amines. We

measured the fluorescence intensity (FL) with fluoraesamine of free amine groups on the product released from enzyme-substrate reaction as product on the SpectraMax M5 (Molecular Devices, MA) at excitation wavelength of 395 and emission at 485 nm.

III. RESULTS

3.3.1 Expression and purification yield of *Mt* MshB

Recombinant MshB from *Mycobacterium tuberculosis* was expressed as fusions to N-terminal 8xHistidine and maltose binding protein (MBP) and in *E. coli* BL21(DE3) ® cells. Cells were induced over night at 20 °C. Soluble protein was purified from cells by a series of chromatographic steps with various yields as summarized (Table 3.1). The identity of all purified proteins, *Mt/Ms* MshB, and *Mt/Ms* MCA, were verified by mass spectrometry (Dr. Keith Ray, Dr. Richard Helm Laboratory, Virginia Tech). After the preparation of apo- *Mt* MshB by treatment with metal chelators, as described in section 3.2.3, the final concentration of proteins was determined with Bradford assay (Table 3.1). The activity of apo-*Ms* MshB after incubation with a variety of metal solutions such as Ni, Co, Mn, Zn and Fe was verified in our laboratory. Results from activity assays for Fe(II) bound

Ms MshB showed the highest activity compared to Zn^{+2} Ni^{+2}, Co^{+2}, Mn^{+2} bound MshB (X. Huang and M. Hernick, unpublished results).

3.3.2 Determination of $K_D^{Zn\ (II)}$ and $K_D^{Fe\ (II)}$ values

We determined the zinc affinities for MshB and MCA using the appropriate zinc buffers using ultra-filtration and analyzed metal ion concentrations in the equal amounts of retentate by IC. Enzyme bound metal fractions were plotted versus free concentration of metal ions in buffers used for the ultra-filtration assay to determine relevant dissociation constant (K_D) values. Here, we showed an example plot of $K_D^{Zn(II)}$ and $K_D^{Fe(II)}$ for Ms MshB (Figure 3. 2). Ultra-filtration experiments shows that $K_D^{Zn(II)}$ values for MshB and MCA pM range such as *Ms* MshB, *Mt* MshB, *Ms* MCA and *Mt* MCA are 360±90 pM, 175±50 pM, 410±70 pM and 220±70 pM, respectively (Table 3.4).In order to determine the dissociation constant of *Ms* MshB for Fe (II), we performed activity assays of apo- *Ms* MshB. We incubated apo- *Ms* MshB with eight different concentrations of Fe (II) buffers in an anaerobic chamber on ice for the enzyme activity assay. We plotted free iron concentration in the buffers against V/Vmax fraction that indicates metal bound enzyme fraction total amount of enzyme using KaleidaGraph software (Figure 3.2). We determined the $K_D^{Fe\ (II)}$ for Ms-MshB as 120 ± 50 nM (Table 3.4).

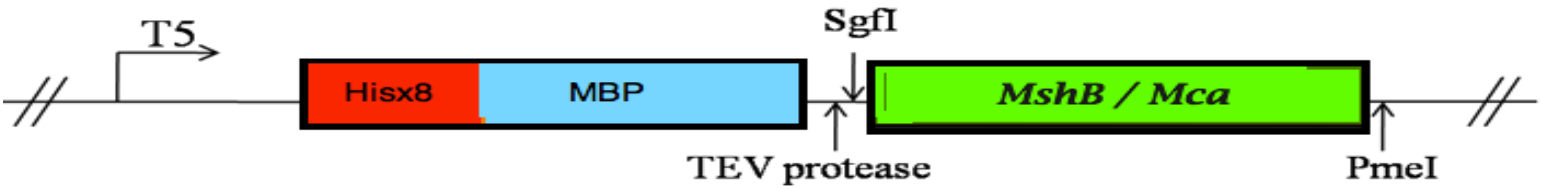

Figure 3.1. Schematic of the pVP56K expression vector

Table 3.1. Results of the expression and purification of apo-*Mt* MshB

Protein content [b]	Final concentration [a]	Expression yield	Total metal
Apo- *Mt* MshB	315uM	(5.16mg/L culture)	<0.02

a. Final concentration of apo-*Mt* MshB, measured by Bradford Assay
b. Total metal content of apo-*Mt* MshB as metal ion per enzyme

Table 3.2. The amounts of total and free iron buffers used in affinity assays

Total Fe [a] (μM)	Free Fe[b] (M)
100	1.19E-08
200	4.23E-08
300	7.15E-08
500	1.62E-07
750	4.64E-07
900	1.33E-06
950	2.67E-06

a. Fe(II) beads (Sigma) were dissolved in metal ion buffer (5 mM Mops,1 mM NTA, pH 7) in a glove box

b. Free concentrations of Fe(II) was calculated by MINEQL+ (Environmental Research Software).

Table 3.3. The amounts of total and free zinc buffers used in affinity assays

Total Zn[a] (μM)	Free Zn[b] (M)
1.00E-09	2.00E-15
5.00E-09	1.06E-14
1.00E-07	2.13E-13
2.50E-07	5.23E-12
5.00E-07	1.06E-12
2.00E-06	4.26E-12
5.00E-06	1.07E-11
2.50E-05	5.46E-11
5.00E-05	1.12E-10
2.00E-04	5.23E-10
5.00E-04	2.13E-09
7.50E-04	6.39E-09
9.00E-04	1.92E-08
9.60E-04	5.10E-08

a. Zn(II) standard (Sigma) were dissolved in metal ion buffer (5 mM Mops, 1 mM NTA, pH 7) in a glove box
b. Free concentrations of Zn(II) was calculated by MINEQL+ (Environmental Research Software).

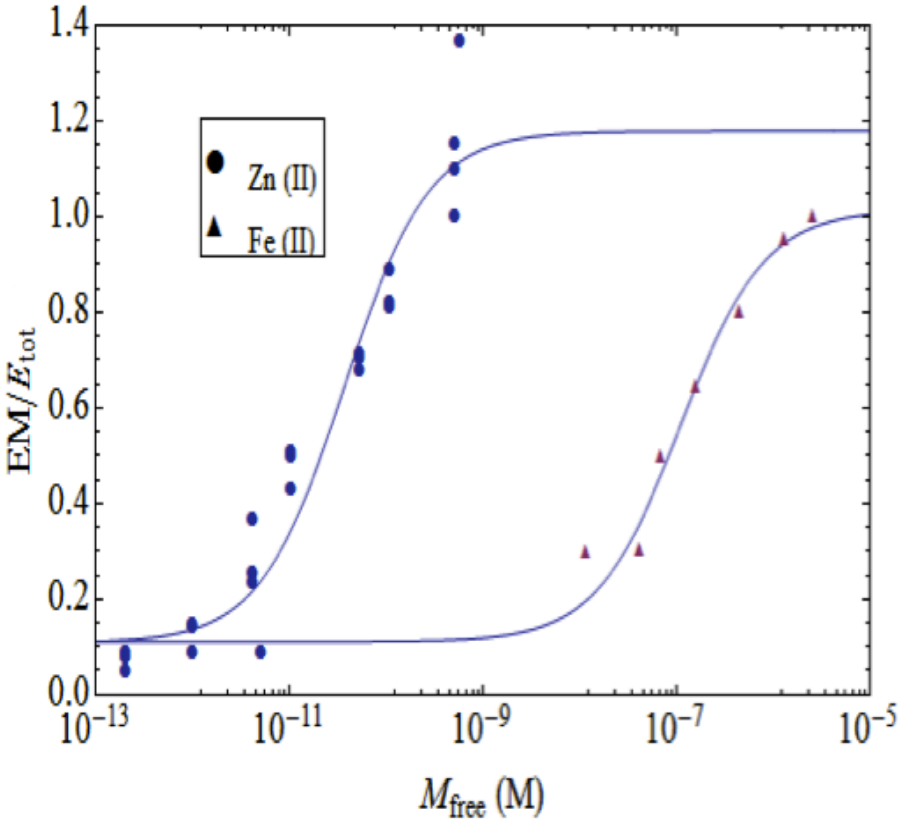

Figure 3.2. $K_D^{Fe(II)}$ and $K_D^{Zn(II)}$ values for *Ms* MshB. $K_D^{Fe(II)}$ and $K_D^{Zn(II)}$ values for *Ms* MshB are 360±90 pM and 120±50nM, respectively. In another word, the affinity of Ms MshB for Zn(II) is 300-fold higher than Fe(II). Apo-*Ms* MshB was encubated with metal solutions (5 mM Mops, 1 mM NTA, pH 7, as described in Section 3.2.4-5). Zn(II) bound MshB (circles) was determined by ultrafiltration and IC analysis (K_DZn). Fe(II) bound MshB (diamonds) was determined by enhancement of the catalytic activity of MshB (K_DFe) measured at 50 mM substrate, 30 °C, pH 7, as described in Section 3.2.5.

Table 3.4. $K_D^{Fe(II)}$ and $K_D^{Zn(II)}$ values for MshB and MCA

Enzyme	$K_D^{Zn(II)}$ [a]	$K_D^{Fe(II)}$ [b]
Ms MshB	360±90 pM	120±50nM
Mt MshB	175±50 pM	N/D[c]
Ms MCA	410±70 pM	N/D[c]
Mt MCA	220±70 pM	N/D[c]

a The affinity of MshB and MCA from *M. smegmatis* and *M. tuberculosis* for Zn(II) was determined using ultrafiltration as described in Section 3.2.4.

b The affinity of MshB and MCA from *M. smegmatis* and *M. tuberculosis* enhanced activity measurements in Fe(II) contained solutions at 30 °C pH 7, as described in Section 3.2.5.

c $K_D^{Fe(II)}$ values fo Mt-MshB, Ms-MCA and Mt-MCA have been not determined yet.

IV.DISCUSSION

3.4.1 Cloning of *Mt* MshB in pPV56K and pPV55A

We generated pVP55A: *Mt* MshB and pVP56K: *Mt* MshB plasmids to express either a His8-*Mt* MshB or His8-MBP-*Mt* MshB. Since *Mt* MshB encoding sequence has an internal restriction Sgf1 site, we first mutated the site *Mt* MshB encoding sequence by using QuickChange® Lightening Site-Directed Mutagenesis Kit (Stratagene, TX) and then followed the steps for Flexi® cloning system as described earlier. Generated pVP55A: *Mt* MshB and pVP56K: *Mt* MshB plasmids sequences were verified at VBI.

3.4.2 Expression, Purification and Preparation of apo-MshB and MCA

We transformed the pVP55A: *Mt* MshB and pVP56K: *Mt* MshB plasmids into the protein expression cell line BL21(DE3)® and expressed the proteins in large scale which refers 4 L LB growth culture amount. Expression levels and solubility of His_8- or His_8-MBP fused *Mt* MshB were visualized on a 12% SDS-PAGE gel by Coomassie staining. Although *Mt* MshB is highly expressed and soluble, MCA cannot be expressed soluble in the absence of MBP (H. Liu and M. Hernick, unpublished results), a well-defined fusion protein that increases solubility.

In general, MBP tag is combined with poly-histidines to be used in metal affinity columns. After Ni-IMAC purification, metal ion contents of *Mt* MshB were analyzed by IC and found that the purified enzyme contains high concentration of nickel (data not shown). In order to carry out metal ion affinity experiments, we further incubated the column-purified proteins with metal chelators to generate apo-enzymes useful for analysis. This process removes almost all metal ions from the enzymes (Total metal content of *Mt* MshB <0.02, Table 3.1).

3.4.3 Determination of $K_D^{Zn(II)}$ and $K_D^{Fe(II)}$ values

In order to understand the metal ion selectivity of *Mt/Ms* MshB and *Mt/* Ms MCA, we determined the affinities of the enzymes for Fe(II) and Zn(II) maintaining the metal concentration with metal ion buffers as described at section 3.2.4 [51]. Determination of the zinc affinity using ultra-filtration and IC analysis show that MshB and MCA from *Mycobacterium tuberculosis* and *Mycobacterium smegmatis* have similar K_D for Zn(II) in pM range (Table 3.4). The dissociation constant of MshB for Fe(II), determined from the enzymatic activity, is the $K_D^{Fe(II)}$ for Ms-MshB is 120 ± 50 nM (Table 3.4).

As mentioned previously, the estimated concentration of total Zn^{2+} and Fe^{2+} per *Mycobacterium tuberculosis* cell is around 37.8±25.2 μM, 505 ±215μM respectively [49,50]. Studies have revealed free Zn(II) and Fe(II) concentrations in mammalian cells, suggest that the concentration of $Zn(II)_{free}$ is 10-400 pM [53,54] while the concentration of $Fe(II)_{free}$ is 0.2-6 μM or higher [55-58]. Although free Zn(II) and Fe(II) concentrations in Mycobacterium species cell have not been determined, yet, it is possible that our determined $K_D^{Fe\ (II)}$ for MshB is lower than the estimated cellular free Fe(II) concentration in *Mycobacterium sp*. Therefore, we could explain that the possible predominance of Fe(II)-MshB *in vivo* based on the fact that the available free Fe(II) concentration could be higher than the K_D^{Fe} for MshB, whereas the available free Zn concentration is close to the K_D^{Zn} value.

Another possible explanation for the possible Fe(II) preference of these enzymes *in vivo*, although Zn(II) has higher affinity for these enzymes than Fe(II); Fe(II) bound MshB and most likely MCA would be the thermodynamically favored form of these enzymes under biological conditions because of the significantly higher concentration of cellular $Fe(II)_{free}$ as suggested in a recent paper from the Fierke's research group [52].

CHAPTER FOUR

CONCLUDING REMARKS AND FUTURE DIRECTIONS

According to recent World Health Organization (WHO) studies, every year almost 2 billion people are infected with tubercle bacilli. Tuberculosis is caused by a group of closely related bacterial species termed the *Mycobacterium tuberculosis* complex (MTBC).

Mycothiol (MSH), a low-molecular- weight thiol, is a primary reducing agent and protects the mycobacterium against oxidative stress. More over, studies indicate that the biosynthesis and detoxification pathway of MSH is necessary for the survival of mycobacteria. The biosynthesis and detoxification pathway of MSH is a six-step process that involves four unique enzymes, MshA, MshA2, MshB, MshC, and MshD and MCA. The identification of the native co-factor is critical for the design of potent and effective inhibitors. The full pathway of MSH biosynthesis and detoxification includes various promising drug targets. In this study, we worked towards to identify native co-factors of two metallohydrolases, which are a deacetylase (MshB) and an amidase (MCA) from *M. smegmatis* and *M. tuberculosis.* MshB catalyzes the deacetylation of GlcNAc-Ins to form GlcN-Ins and acetate. Mycothiol *S*-conjugate amidase (MCA) cleaves

the amide bond of mycothiol *S*-conjugates of various drugs and toxins and leads the product exported from the cell as a mercupturic acid.

Previous studies demonstrated that divalent metals could activate MshB and MCA [39]. However, in the studies the ability of Fe^{2+} to activate MshB was not examined. Our laboratory observed that apo-MshB shows higher activity when it is bound Fe^{2+} than bound Zn^{2+}. Moreover, Fe^{2+} bound MshB is oxygen sensitive. In another word, Fe^{2+} bound MshB loses its activity under aerobic conditions depending on time. (X. Huang and M. Hernick, unpublished results)

It is known that Fe^{2+} oxidizes to Fe^{3+} very quickly and possibly, replaced by Zn^{2+} in the active site; as a result, the native metal cofactor of aerobically purified enzymes could be misidentified as Zn^{2+}·Recent studies have re-classified several "Zn^{2+}-dependent" enzymes as "Fe^{2+}-dependent" enzymes, including peptide deformylase (PDF) LuxS, histone deacetylase 8 (HDAC8) and LpxC.

In this study, we aimed to determine the presence of iron (II) *in vivo* conditions. To reach our aim, we used a rapid purification method, as referred pull-down experiments, which allowed us to isolate recombinant MshB and MCA. The encoding sequences for MshB and MCA were fused

to N-terminal HaloTag® and expressed in chemically defined medium supplemented with iron or zinc or both, in E.coli. We carried out the purification of MshB and MCA under aerobic and anaerobic conditions.

Our data indicates that the metal bound to MshB and MCA anaerobically purified from *E. coli* grown in minimal medium is mainly Fe(II). Moreover, MshB and MCA can be found bound Zn(II), some Fe(II) after their aerobic purification.

Determination of metal ion affinities of MshB and MCA is important to clarify the data from pull-down experiments in order to understand the possible reasons that enzymes prefer to be bound iron or zinc. One possibility is that we observed Fe(II) bound these enzymes due to it has higher affinity than Zn(II). Another possibility could be that enzymes prefer Fe(II) *in vivo.* In addition, it is possible that enzymes use multiple co-factors to regulate their physiologic activities under different environmental conditions by using a metal switching mechanism.

We determined the MshB and MCA affinity for Zn(II) to be in the picomolar range and *Ms* MshB affinity for Fe(II) in nanomolar range. These results indicate that MshB and MCA can be found bound with either iron or zinc and this is independent to their affinities for these metal ions.

In order to clarify the metal ion preferences of MshB and MCA the exchange rates of Fe/ Zn from the enzymes will be measured. Apo-enzyme, first, incubated with iron buffer then a second incubation of Fe bound enzyme with a zinc buffer to determine the rate of metal ion exchange in the enzyme active site. Results from this experiment can provide an insight that a possible metal switching occurrence in the enzyme active site.

As mentioned earlier, in this study we performed the experiments with recombinant proteins expressed in *E.coli*. Performing the similar pull-down experiments with *Mycobacterium* sp. would provide more precise understanding the native co-factor of MshB and MCA in their natural environment.

REFERENCE LIST

1. Donoghue, H.D., *Human tuberculosis - an ancient disease, as elucidated by ancient microbial biomolecules*. Microbes Infect, 2009. **11**(14-15): p. 1156-62.
2. World Health Organization, *2009 Update Turbeculosis Facts* [cited 2010 July 23]; Available from: http://www.who.int/tb/publications/2009/factsheet_tb_2009update_dec09.pdf.
3. World Health Organization, *Global Turbeculosis Control – a short update to the 2009 report* [cited 2010 July 23]; Available from: http://whqlibdoc.who.int/publications/2009/9789241598866_eng.pdf.
4. Gordon, S.V., et al., *Pathogenicity in the tubercle bacillus: molecular and evolutionary determinants*. BioEssays, 2009. **31**(4): p. 378-8.
5. Ventura, M., et al., *Genomics of Actinobacteria: tracing the evolutionary history of an ancient phylum*. Microbiol Mol Biol Rev, 2007. **71**: p. 495-548.
6. Kalinowski, J., et al.. *The complete Corynebacterium glutamicum ATCC 13032 genome sequence and its impact on the production of L-aspartate-derived amino acids and vitamins*. J Biotechnol, 2003. **104**: p. 5-25.
7. Weber, T., et al., *Exploiting the genetic potential of polyketide producing streptomycetes*. J Biotechnol, 2003. **106**: p. 221-32.
8. World Health Organization, *Anti-turbeculosis drug resistance in the world* [cited 2010 July 23]; Available from: http://www.who.int/tb/publications/2008/drs_report4_26feb08.pdf
9. Crofton, J., *Chemotherapy of pulmonary tuberculosis*. Br Med J, 1959. **1**: p. 1610–14.

10. Global Alliance for Tuberculosis Drug Development, *Executive Summary of the Scientific Blueprint for TB Drug Development*, 2001. [cited 2010 July 23]; Available from: http://www.tballiance.org/downloads/publications/TBA_Scientific_Blueprint.pdf
11. Zhang, Y., *The magic bullets and tuberculosis drug targets*. Annu Rev Pharmacol Toxicol, 2005. **45**(1): p. 529-64.
12. Newton, G.L., et al., *Distribution of thiols in microorganisms: mycothiol is a major thiol in most actinomycetes*. J Bacteriol, 1996. **178**(7): p. 1990-95.
13. Masip, L., et al., *The many faces of Glutathione in bacteria*. Antioxid Redox Signal, 2006. **8**: p. 753–62.
14. Newton, G.L., et al., *Low-molecular-weight thiols in streptomycetes and their potential role as antioxidants*. J Bacteriol, 1993. **175**(9): p. 2734-42.
15. Bornemann, C., et al., *Biosynthesis of mycothiol: elucidation of the sequence of steps in Mycobacterium smegmatis*. Biochem J, 1997. **325**(3): p. 623-9.
16. Penninckx, M. J. and M.T. Elskens, *Metabolism and functions of glutathione in micro-organisms.* Adv Microb Physiol, 1993. **34**: p. 239–301.
17. Sareen, D., et al., *Mycothiol Is Essential for Growth of Mycobacterium tuberculosis Erdman*. J Bacteriol, 2003. **185**(22): p. 6736-40.
18. Buchmeier, N. and R.C. Fahey. *The mshA gene encoding the glycosyltransferase of mycothiol biosynthesis is essential in Mycobacterium tuberculosis Erdman*. FEMS Microbiol Lett, 2006. **264**(1): p. 74-9.

19. Rawat, M., et al., *Mycothiol-deficient Mycobacterium smegmatis mutants are hypersensitive to alkylating agents, free radicals, and antibiotics*. Antimicrob Agents Chemother, 2002. **46**(11): p. 3348-55.
20. Koledin, T, et al., *Identification of the mycothiol synthase gene (mshD) encoding the acetyltransferase producing mycothiol in actinomycetes.* Arch Microbiol, 2002. **178**(5): p.331-7.
21. Newton, G.L., et al., *The Glycosyltransferase Gene Encoding the Enzyme Catalyzing the First Step of Mycothiol Biosynthesis (mshA)*. J Bacteriol, 2003. **185**(11): p. 3476-9.
22. Rawat, M., et al., *Inactivation of mshB, a key gene in the mycothiol biosynthesis pathway in Mycobacterium smegmatis.* Microbiology, 2003. **149**: 1341-9.
23. Newton, G.L., et al., *Biochemistry of the Initial Steps of Mycothiol Biosynthesis*. J Biol Chem, 2006. **281**(45): p. 33910-20.
24. Newton, G.L., et al., *N-Acetyl-1-D-myo-Inosityl-2-amino-2-deoxy-alpha-D-glucopyranoside deacetylase (MshB) is a key enzyme in mycothiol biosynthesis.* J Bacteriol, 2000. **182**(24): p. 6958-63.
25. Koledin, T, et al., *Identification of the mycothiol synthase gene (mshD) encoding the acetyltransferase producing mycothiol in actinomycetes.* Arch Microbiol, 2002. **178**(5): p.331-7.
26. Newton et al. *A novel mycothiol-dependent detoxification pathway in mycobacteria involving mycothiol S-conjugate amidase*. Biochem, 2000. **39**(35): p. 10739-46.
27. Buchmeier N.A,, et al., *Association of mycothiol with protection of Mycobacterium tuberculosis from toxic oxidants and antibiotics*. Mol Microbiol, 2003. **47**(6): p. 1723-32.

28. Maynes, J.T., et al., *The Crystal Structure of 1-D-myo-inosityl 2-acetamido-2-deoxy-alpha-D-glucopyranoside deacetylase (MshB) from Mycobacterium tuberculosis reveals a zinc hydrolase with a lactate dehydrogenase fold.* J Biol Chem, 2003. **278**: p. 47166-70.
29. McCarthy, A.A., et al., *Crystal Structure of MshB from Mycobacterium tuberculosis, a deacetylase involved in mycothiol biosynthesis*. J Mol Biol, 2004. **335**(4): p. 1131-41.
30. Newton, G.L., et al., *Purification and characterization of Mycobacterium tuberculosis 1-D-myo-inosityl-2-acetamido-2-deoxy-alpha-d-glucopyranoside deacetylase, MshB, a mycothiol biosynthetic enzyme.* Protein Expr Purif, 2006. **47**(2): p. 542-50.
31. Metaferia, B.B., et al., *Synthesis of Natural Product-Inspired Inhibitors of Mycobacterium tuberculosis Mycothiol-Associated Enzymes: The First Inhibitors of GlcNAc-Ins Deacetylase.* J Med Chem, 2007. **50**(25): p. 6326-36.
32. Chasseaud, L.F., *Conjugation with glutathione and mercapturic acid excretion*, in I. M. Arias and W. B. Jakoby (ed.), *Glutathione: metabolism and function*, 1976. Raven Press, New York, NY, p. 77-114.
33. Stevens, J.L., and D.P. Jones, *The mercapturic acid pathway: biosynthesis, intermediary metabolism, and physiological disposition*, in *Glutathione: Chemical, Biochemical, and Medical Aspects, Part B,* 1989. Dolphin, D., Poulson, R., and Avramovic, O. (eds.), John Wiley, New York, p. 45-84.
34. Rawat, M. and Y. Av-Gay, *Mycothiol-dependent proteins in actinomycetes*. FEMS Microbiol Rev, 2007. **31**(3): p. 278-92.
35. Steffek, M., et al., *Characterization of Mycobacterium tuberculosis Mycothiol S-Conjugate Amidase*. Biochem, 2003. **42**(41): p. 12067-76.

36. Newton, G.L. and R.C. Fahey, *Mycothiol biochemistry*. Arch Microbiol, 2002. **178**(6): p. 388-94.
37. Jothivasan, V.K. and C.J. Hamilton, *Mycothiol: synthesis, biosynthesis and biological functions of the major low molecular weight thiol in actinomycetes*. Nat Prod Rep, 2008. **25**(6): p. 1091-117.
38. Roe, R.R., and Y.P. Pang, *Zinc's exclusive tetrahedral coordination governed by its electronic structure*, J Mol Model, 1999. **5**: p. 134-40.
39. Auld, D.S., *Removal and replacement of metal ions in metallopeptidases*, Methods Enzymol, 1995. **248**: p. 228-42.
40. Nicholas, G.M., et al., *Inhibition and kinetics of mycobacterium tuberculosis and mycobacterium smegmatis mycothiol-S-conjugate amidase by natural product inhibitors*. Bioorg Med Chem, 2003. **11**(4): p. 601-8.
41. Nicholas, G.M., et al., *Bromotyrosine-Derived Natural and Synthetic Products as Inhibitors of Mycothiol-S-Conjugate Amidase*. Bioorg Med Chem Lett, 2002. **12**(17): p. 2487-90.
42. Groche, D. , et al., *Isolation and crystallization of functionally competent Escherichia coli peptide deformylase forms containing either iron or nickel in the active site.* Biochem Biophys Res Commun, 1998. **246**: p. 342-6.
43. Rajagopalan, P.T.R. , et al., *Peptide deformylase: A new type of mononuclear iron protein.* J Am Chem Soc, 1997. **119**: p. 12418-9.
44. Becker, A., et al., *Iron center, substrate recognition and mechanism of peptide deformylase.* Nat Struct Biol, 1998, **5**: p. 1053-58.
45. Zhu, J.G., et al., *S-Ribosylhomocysteinase (LuxS) is a mononuclear iron protein*, Biochem, 2003. **42**: p. 4717-26.
46. Gantt, S.L., et al., *Catalytic activity and inhibition of human histone*

deacetylase 8 is dependent on the identity of the active site metal ion. Biochem, 2006. **45**: p. 6170-8.

47. Hernick, M., et al., *Activation of Escherichia coli UDP-3-O-[(R)-3-hydroxymyristoyl]-N-acetylglucosamine Deacetylase by Fe2+ Yields a More Efficient Enzyme with Altered Ligand Affinity*. Biochem, 2010. **49**(10): p. 2246-55.

48. Jackman, J. E., et al., *UDP-3-O-(R-3-hydroxymyristoyl)-N-acetylglucosamine deacetylase of Escherichia coli is a zinc metalloenzyme.* Biochem, 1999. **38**: p. 1902-11.

49. Outten, C.E. and T.V. O'Halloran, *Femtomolar Sensitivity of Metalloregulatory Proteins Controlling Zinc Homeostasis.* Sci, 2001. **292** (5526): p. 2488-92.

50. Wagner, D., et al., *Elemental Analysis of Mycobacterium avium-, Mycobacterium tuberculosis-, and Mycobacterium smegmatis-Containing Phagosomes Indicates Pathogen-Induced Microenvironments within the Host Cell's Endosomal System*. J Immunol, 2005. **174**(3): p. 1491-500.

51. Bozym,R., et al., *Determination of zinc using carbonic anhydrase-based fluorescence biosensors.* Methods Enzymol, 2008. **450**: p. 287-309.

52. Samuel G., et al., *Metal switching between Fe(II) and Zn(II) as a mechanism of regulation of UDP-3-0-(R-3-hydroxymyristoyl)-N-acetylglucoamine deacetylase.* Biochem, 2010**. 49**(10): p. 2246–55.

53. Bozym, R. A., et al*., Measuring picomolar intracellular exchangeable zinc in PC-12 cells using a ratiometric fluorescence biosensor.* ACS Chem Biol, 2006**. 1**(2): p. 103-111.

54. Vinkenborg, J. L., et al., *Genetically encoded FRET sensors to monitor intracellular Zn^{2+} homeostasis.* Nat Methods, 2009. **6**(10): p. 737-40.

55. Petrat, F., et al., *Subcellular distribution of chelatable iron: a laser scanning microscopic study in isolated hepatocytes and liver endothelial cells*. Biochem J, 2001. **356**(1): p. 61-9.

56. Espósito, B. P., et al., *A review of fluorescence methods for assessing labile iron in cells and biological fluids.* Anal Biochem, 2002. **304**(1): p. 1-18.

57. Meguro, R., et al., *Nonheme-iron histochemistry for light and electron microscopy: a historical, theoretical and technical review*. Arch Histol Cytol, 2007. **70**(1): p. 1-19.

58. MacKenzie, E. L., et al., *Intracellular iron transport and storage: From molecular mechanisms to health implications.* Antioxid Redox Signal, 2008. **10**(6): p. 997-1030.

59. Ohana et al.,*HaloTag7: A genetically engineered tag that enhances bacterial expression of soluble proteins and improves protein purification,* Protein Expression and Purification, 2009.(68):p.110-120

60. Outten, F.W., et al., *Transcriptional activation of an Escherichia coli copper efflux regulon by the chromosomal MerR homologue, CueR.* J Biol Chem, 2000. **275**(40): p. 31024-9.

61. Qi and Scholthof. *A one-step PCR-based method for rapid and efficient site- directed fragment deletion, insertion, and substitution mutagenesis*. Journal of Virological Methods (2008) vol. 149 (1) pp. 85-90